PHASE RESETTING IN A MODEL OF CARDIAC PURKINJE FIBER

MICHAEL R. GUEVARA AND ALVIN SHRIER
Department of Physiology, McGill University, Montreal, Quebec, Canada H3G 1Y6

ABSTRACT The phase-resetting response of a model of spontaneously active cardiac Purkinje fiber is investigated. The effect on the interbeat interval of injecting a 20-ms duration depolarizing current pulse is studied as a function of the phase in the cycle at which the pulse is delivered. At low current amplitudes, a triphasic response is recorded as the pulse is advanced through the cycle. At intermediate current amplitudes, the response becomes quinquephasic, due to the presence of supernormal excitability. At high current amplitudes, a triphasic response is seen once more. At low stimulus amplitudes, type 1 phase resetting occurs; at medium amplitudes, a type could not be ascribed to the phase resetting because of the presence of effectively all-or-none depolarization; at high amplitudes, type 0 phase resetting occurs. The modeling results closely correspond with published experimental data; in particular type 1 and type 0 phase resetting are seen. Implications for the induction of ventricular arrhythmias are considered.

INTRODUCTION

Injection of a current pulse into a spontaneously beating cardiac Purkinje fiber causes a transient change in its beat rate leading to a permanent phase-resetting of its rhythm (Weidmann, 1951, 1955a; Jalife and Moe, 1976, 1979; Jalife and Antzelevitch, 1980; Antzelevitch et al., 1982). While there have been a few modeling studies of Purkinje fiber that dealt incidentally with the effect of injecting a current pulse (Hauswirth, 1971; McAllister et al., 1975; DiFrancesco and Noble, 1982; Drouhard and Roberge, 1982), there appears to have been only one study in which phase-resetting per se was systematically investigated (Chay and Lee, 1984). However, that report modeled a Purkinje fiber in which a constant bias current had been injected, and focused on the annihilation of spontaneous activity that can be produced by a single current pulse in that circumstance. We describe below the phase-resetting behavior of an unmodified model of Purkinje fiber. Our main interest in doing so is to investigate the topology of phase resetting. This is a necessary first step in determining the extent to which the phase-resetting response (produced by injecting a single current pulse) might account for the response to periodic stimulation with a train of such current pulses.

METHODS

The model of Purkinje fiber investigated in this report is the MNT model (McAllister et al., 1975). Numerical integration was carried out in single precision (approximately seven significant decimal digits) using an efficient variable time-step algorithm, the convergence of which can be

Address correspondence to A. Shrier, Department of Physiology, McGill University, 3655 Drummond Street, Montreal, Quebec, Canada H3G 1Y6.

analytically shown (Victorri et al., 1985). The maximum change in the transmembrane potential ΔV allowed in iterating from time t to time $t + \Delta t$ was 0.4 mV. When a value of ΔV larger than this upper limit resulted, the integration time step Δt was successively halved and the calculations redone until ΔV was <0.4 mV. When ΔV was <0.2 mV, Δt was doubled for the following iteration. We found, with one exception mentioned below, that allowing Δt to lie in the range 0.001 ms $\leq \Delta t \leq$ 8.192 ms permitted ΔV to remain below 0.4 mV when a current pulse was injected. Under these conditions, the voltage waveform during spontaneous activity is within a few percent of that obtained using a very accurate Runge–Kutta fourth-order integration scheme using a fixed Δt of 0.005 ms (Victorri et al., 1985). In advancing from time t to time $t + \Delta t$, the contribution of the membrane current to ΔV was calculated using the fomula appearing in footnote 2 of Victorri et al. (1985). The time step Δt was adjusted when a current pulse was delivered so that the current started and stopped at exactly the right times. Initial conditions, unless otherwise stated, were as follows: $V = -80.00$ mV, $m = 0.01946$, $h = 0.8591$, $d = 0.002089$, $f = 0.7725$, $x_1 = 0.02694$, $x_2 = 0.01986$, $q = 2.156 \times 10^{-6}$, $r = 0.1190$, and $s = 0.7791$. The initial value of Δt was 0.512 ms. These initial conditions closely approximate a point on the limit cycle. L'Hôpital's rule was applied when necessary in calculating the rate constants α_m, α_d, α_q, and α_s as well as the current I_{K_1}. We have used Eqs. 25 and 26 rather than Eqs. 27 and 28 of McAllister et al. (1975) to describe α_r. Finally, there is an inconsistency in the paper of McAllister et al. (1975), which was earlier pointed out by Chay and Lee (1984), between the formula for α_f given first in Table 1A and then repeated later in the text in Eq. 16. We have used the latter formula, since using the one in Table 1A leads to such a large window current for I_{si} that spontaneous activity does not occur. In addition, the current–voltage characteristics are then very close to those shown in Figs. 1–3 of McAllister et al. (1975).

RESULTS

Fig. 1 shows the effect of injecting a 20-ms duration depolarizing current pulse of magnitude 4 $\mu A/cm^2$: either a prolongation or abbreviation of the interbeat interval results, depending upon whether the stimulus is delivered relatively early (Fig. 1, *middle*) or late (Fig. 1, *bottom*) in the cycle. We define the interbeat interval to be the time
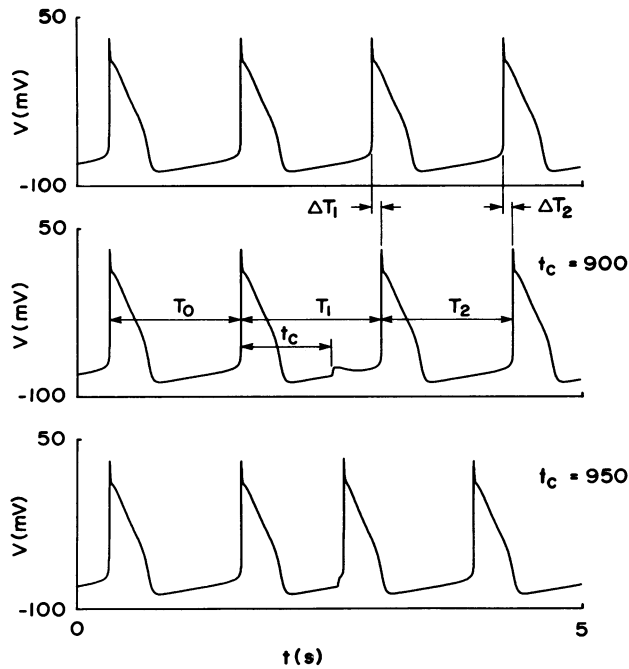
FIGURE 1 The phase-resetting effect of injecting a depolarizing current pulse of duration 20 ms and amplitude 4 μA/cm^2 at a coupling interval of t_c = 900 ms (*middle*) and t_c = 950 ms (*bottom*). Unperturbed activity is seen at top. In this and subsequent figures, the number appearing to the side of the trace is the coupling interval t_c in milliseconds.

between successive crossings of -10 mV on the action potential upstroke. This "event marker" point approximates the location of the maximal upstroke velocity in the MNT model (McAllister et al., 1975). We denote the spontaneous interbeat interval by T_0 (which we take to be 1306.668 ms), the perturbed interbeat interval (the duration of the cycle in which the stimulus occurs) by T_1, and the post-stimulus interbeat interval (the duration of the cycle immediately after the perturbed cycle) by T_2 (Fig. 1, *middle*). The coupling interval of the stimulus pulse is defined to be the time from the crossing of -10 mV on the upstroke of the action potential immediately before the pulse to the time of onset of the pulse, and is denoted by t_c. All intervals are given in milliseconds. The phase ϕ ($0 \leq \phi < 1$) in the cycle at which the stimulus falls is defined by $\phi = t_c/T_0$. The stimulus amplitude in μA/cm^2 is denoted by A, with a positive value of A corresponding to a depolarizing stimulus.

One can also define the temporal shifts (Fig. 1)

$$\Delta T_1 = T_0 - T_1 \qquad (1)$$

and

$$\Delta T_2 = 2T_0 - (T_1 + T_2). \qquad (2)$$

Similarly, for $i > 2$, $\Delta T_i = i \cdot T_0 - \Sigma_{j-1}^{i} T_j$. Note that the sign of ΔT_1 is positive if $T_1 < T_0$ ("advance") and negative if $T_1 > T_0$ ("delay"). Note also that at the amplitude of stimulation used in Fig. 1, $T_2 \simeq T_0$, and so $\Delta T_2 \simeq \Delta T_1$. This

is not the case at higher stimulus amplitudes considered below, when T_2 can differ significantly from T_0, and ΔT_2 can therefore be quite different from ΔT_1.

We have systematically investigated the effect of injecting a 20-ms duration depolarizing current pulse at amplitudes from 1 to 15 μA/cm^2 in steps of 1 μA/cm^2. At each of these amplitudes, the coupling interval t_c was changed with an increment of 10 ms (a "phase-resetting run"). Fig. 2 shows voltage tracings selected out of such runs carried out at three different current amplitudes lying at the lower end of the amplitude range investigated. Fig. 3 summarizes the findings, plotting the normalized perturbed interbeat interval T_1/T_0 as a function of the normalized coupling interval $\phi = t_c/T_0$, with an increment in t_c of 10 ms.

In Fig. 3, for t_c = 150 ms at A = 4 μA/cm^2 and for t_c = 150, 160, and 170 ms at A = 6 μA/cm^2, the voltage crosses -10 mV during the time that current is being injected. However, since the membrane resumes repolarizing once
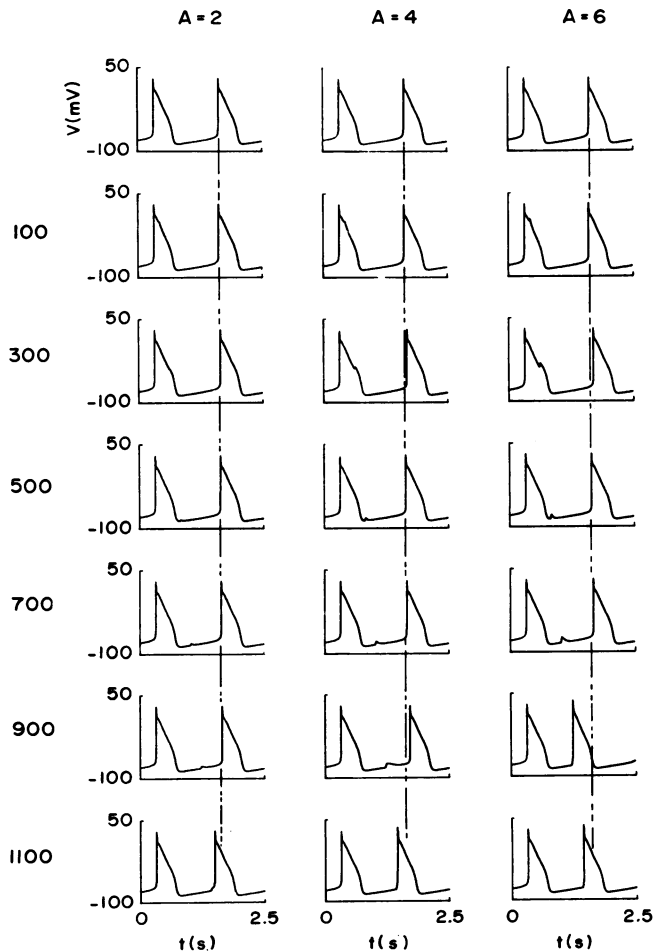

FIGURE 2 Phase-resetting effect of injecting a single 20-ms duration depolarizing current pulse of amplitude 2 μA/cm^2 (*left*), 4 μA/cm^2 (*middle*), and 6 μA/cm^2 (*right*). The uppermost trace in all three panels shows a cycle of unperturbed activity; the dashed line running through each panel indicates the unperturbed cycle length. The coupling interval t_c increases from 100 to 1,100 ms in 200-ms steps from the second to the last row.
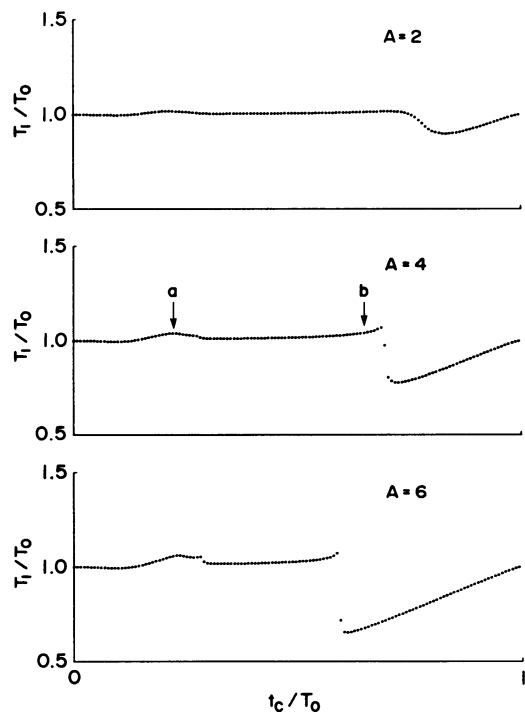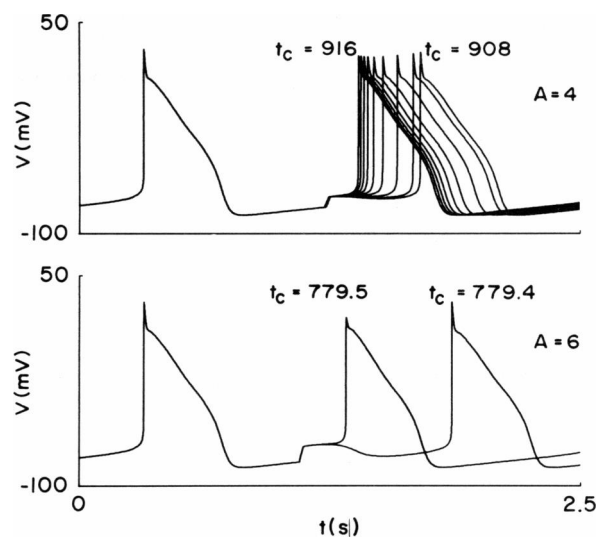
FIGURE 4 Effect of changing the coupling interval t_c in 1.0-ms steps from $t_c = 908$ ms to $t_c = 916$ ms at a pulse amplitude of 4 μA/cm^2 (top) and in a 0.1-ms step from $t_c = 779.4$ ms to $t_c = 779.5$ ms at a pulse amplitude of 6 μA/cm^2 (bottom).

FIGURE 3 The normalized perturbed interbeat interval T_1/T_0 plotted against the normalized coupling interval t_c/T_0 at each of the three different pulse amplitudes shown in Fig. 2. The coupling interval is changed in 10-ms steps from 0 to 1,600 ms inclusive. Pulse amplitude: 2 μA/cm^2 (top), 4 μA/cm^2 (middle), 6 μA/cm^2 (bottom). The arrows (middle) indicate the two well-separated ranges of coupling interval over which prolongation occurs. There is also a very slight abbreviation of cycle length for stimuli falling very early in the cycle, which is not too evident on the scale of this diagram.

the pulse is turned off (producing a waveform resembling that shown in Fig. 2, right; $t_c = 300$ ms), an action potential upstroke has not occurred and we have not accepted the crossing of -10 mV as the second event marker for establishing the value of T_1. Instead, we have waited until the next crossing of -10 mV, which occurs on the first action potential upstroke after the current pulse is turned off.

Fig. 3 indicates that the transition from prolongation to abbreviation of interbeat interval takes place with a very small change in t_c (10 ms) at $A = 4$ μA/cm^2 and at $A = 6$ μA/cm^2. Fig. 4 investigates this transition at these two levels using finer increments in t_c. At $A = 4$ μA/cm^2 (Fig. 4, top), an increment in t_c of 1.0 ms is sufficient to reveal the existence of intermediate responses spanning the entire range from maximal prolongation to maximal abbreviation of interbeat interval; at $A = 6$ μA/cm^2 (Fig. 4, bottom), an increment one-tenth as large (i.e., 0.1 ms) is not sufficient to reveal whether or not these intermediate responses exist. As the stimulus amplitude is increased beyond 6 μA/cm^2, the transition occurs at a smaller coupling interval and is even more abrupt.

Over a range from $A \simeq 7$ μA/cm^2 to $A \simeq 11$ μA/cm^2, the gap phenomena is observed (Agha et al., 1973). Graded

action potentials are seen as t_c is incremented during the repolarization phase (e.g., Fig. 5, left; $A = 10$ μA/cm^2; $t_c = 400$ ms); at larger values of t_c, action potentials are not elicited (e.g., Fig. 5, left; $t_c = 450$ and 500 ms); for t_c sufficiently large, action potentials are once again seen (e.g., Fig. 5, left; $t_c = 550$ and 600 ms). This gap phenomena results in supernormal excitability (see Discussion).

As the pulse amplitude is increased in the range where the gap phenomenon occurs, the size of the gap, i.e., the range of t_c over which it exists, first increases but then decreases. In fact, at $A = 12$ μA/cm^2, the gap phenomenon is not seen when t_c is changed in steps of 10 ms; instead, the graded action potential produced by premature stimulation early in the cycle simply tends to grow in amplitude and duration as t_c is increased (Fig. 5, right). In fact, there is a range of t_c over which the overshoot potential becomes more positive than during unperturbed activity (e.g., Fig. 5, right; $t_c = 450$–600 ms). The voltage waveforms seen during phase resetting do not change qualitatively from those shown in the right panel of Fig. 5 as the pulse amplitude is further increased (at least up to $A = 50$ μA/cm^2).

Fig. 6 shows, using a finer increment in t_c than that used in the right panel of Fig. 5, responses seen at $A = 12$ μA/cm^2 for values of t_c in a neighborhood of that at which graded action potentials first appear as t_c is increased. Note that the waveforms change in a smoothly continuous manner, with no sign of an abrupt transition as the graded action potential makes its appearance. Note also that the membrane potential at the end of the current pulse lies in the plateau range of potentials when graded action potentials begin to appear.
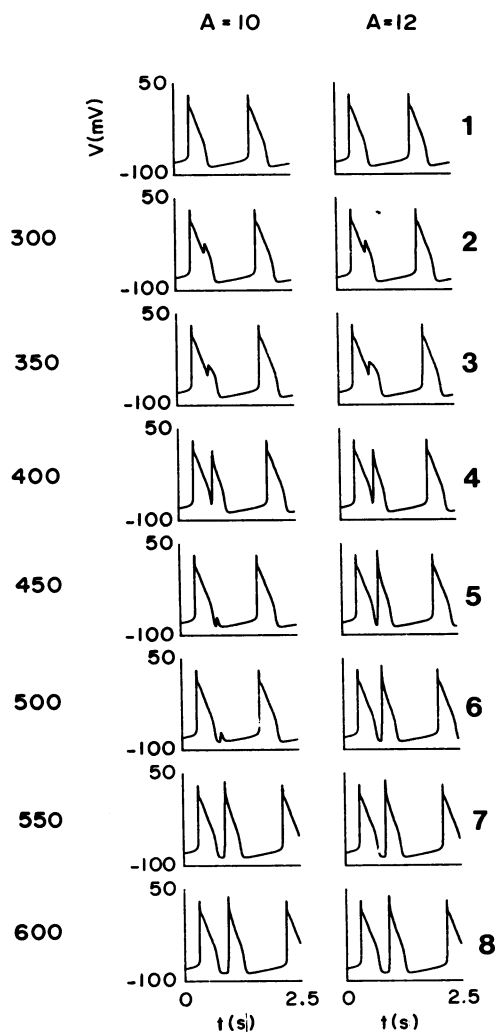
FIGURE 5 Effect of changing the coupling interval t_c in 50-ms steps from t_c = 300 ms (row 2) to t_c = 600 ms (row 8) at each of two pulse amplitudes: 10 μA/cm^2 (left) and 12 μA/cm^2 (right). Row 1 shows unperturbed activity.

Fig. 6 also illustrates that there can be severe methodological problems when applying the definition of the interbeat interval T_1. For example, using our definition of the event marker, the upstroke phase of the waveform appearing at t_c = 380 ms would not be classified as an event, since its overshoot potential is more negative than
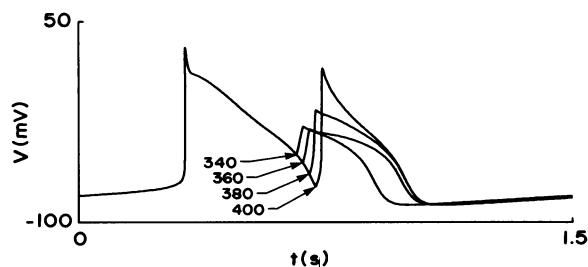

FIGURE 6 Part of phase-resetting run earlier shown in the right panel of Fig. 5 (pulse amplitude, 12 μA/cm^2). The increment in t_c is now 20 ms, with t_c between 340 and 400 ms.

-10 mV and thus the upstroke phase does not cross -10 mV. Yet, there is some form of "active" response, in that the membrane continues to depolarize after turnoff of the current pulse; indeed, there is considerably more depolarization during this current pulse than at $t_c \leq 360$ ms. At t_c = 400 ms, the upstroke crosses -10 mV and so, by our definition, an event occurs. We have explored the consequences of several alternative definitions of the event marker (e.g., a local maximum in the membrane potential); however, all have one form or another of methodological shortcoming.

Fig. 7 is a graphical summary of our phase-resetting results over the entire range of qualitatively different behaviors encountered. In Fig. 7, left, the normalized perturbed interbeat interval T_1/T_0 is plotted as a function of the normalized coupling interval $\phi = t_c/T_0$ with t_c being changed in steps of 10 ms. Unlike the case in Fig. 3, we have adhered strictly to our definition of T_1, taking any positive-going crossing of -10 mV as an event. This produces artifacts, such as the shortenings of T_1 seen at small values of ϕ in all rows (except the first) of Fig. 7; for example, the arrow labeled a in the third row (A = 6 μA/cm^2) indicates a segment of data where this effect is present.

We now turn to consideration of topological aspects of phase resetting (see Appendix for background). Using the definition

$$\phi_1' = \phi + \Delta T_1/T_0 \text{ (modulo 1)}, \qquad (3)$$

where ΔT_1 is as defined in Eq. 1 and Fig. 1 above, the "first transient phase" ϕ_1' can be plotted against the "old phase" ϕ (Fig. 7, middle). A curve drawn through the data points is called the first transient phase transition curve (Pavlidis, 1973; Winfree, 1980; Kawato, 1981), abbreviated PTC$_1$. Similarly, the "second transient phase" ϕ_2' (Fig. 7, right) can be calculated from the definition

$$\phi_2' = \phi + \Delta T_2/T_0 \text{ (modulo 1)}, \qquad (4)$$

where ΔT_2 is as defined in Eq. 2 and Fig. 1 above. Calculation of the third transient phase ϕ_3' results in data points that superimpose with those of ϕ_2' shown in the right panel of Fig. 7. The state-point of the system has thus effectively returned to the limit cycle by that time: PTC$_2$ can therefore be taken as a very good approximation to PTC$_\infty$.

For a current amplitude smaller than $\sim$4 μA/cm^2, PTC$_2$ is a continuous curve with an average slope of one (e.g., Fig. 7, rows 1 and 2): its topological degree is one, and type 1 phase resetting is said to occur (Winfree, 1980). For $A \geq$ 12 μA/cm^2, PTC$_2$ also appears to be a continuous curve when t_c is changes in 10-ms steps (e.g., Fig. 7, rows 5 and 6); however, its average slope is zero, its topological degree is zero, and type 0 phase resetting exists (Winfree, 1980). Note also that for $A \leq 3$ μA/cm^2, PTC$_2$ is of degree one and monotonically increasing (e.g., Fig. 7, row 1), but that for A above this value, PTC$_2$ is no longer monotonically
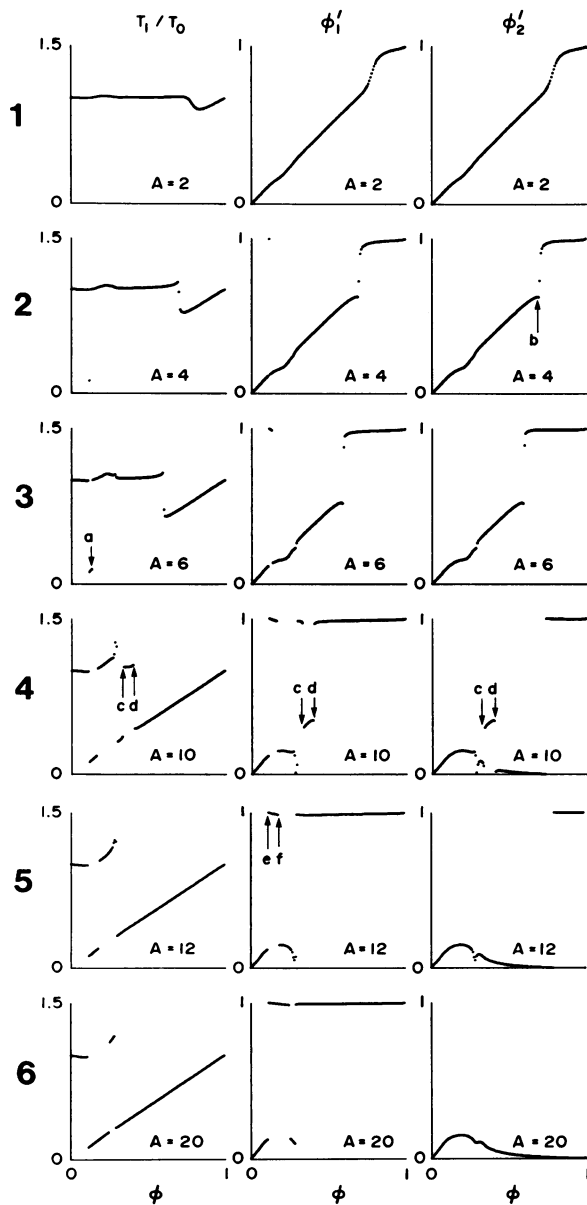
FIGURE 7 The normalized perturbed interbeat interval T_1/T_0 (left), the first transient phase ϕ_1' (middle), and the second transient phase ϕ_2' (right) plotted against the old phase ϕ at, from top to bottom, pulse amplitudes of 2, 4, 6, 10, 12, and 20 μA/cm^2. The increment in t_c is 10 ms. At $A = 20$ μA/cm^2, it was necessary to decrease the minimum value of the integration time step Δt from its usual value of 1.0 μs to 0.5 μs to permit the maximum value of the change in voltage ΔV to remain below 0.4 mV (see Methods). The arrows labeled a–f indicate features of the curves discussed in the text.
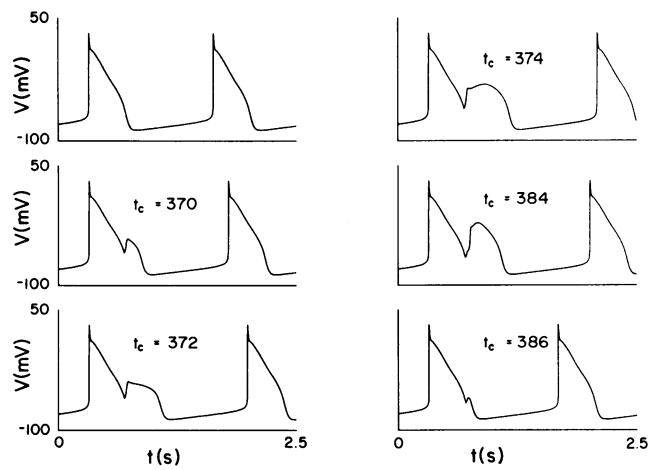

FIGURE 8 Effect of changing the coupling interval t_c at a pulse amplitude (7 μA/cm^2) near where graded action potentials are first seen. Note the long-drawn-out response at $t_c = 374$ ms. The top trace at left shows unperturbed activity.

Note that in all but the first row of Fig. 7, PTC$_1$ shows discontinuities that are not visible on PTC$_2$ (e.g., Fig. 7, row 5; at $\phi \simeq 0.11$ [arrow labeled e] and at $\phi \simeq 0.18$ [arrow labeled f]). These discontinuities are artifacts because one must adhere to an arbitrary, but precise, definition of an event marker in determining the ΔT_i used in calculating the ϕ_i'. These discontinuities appear to be a compulsory feature of phase-resetting, but are expected to disappear in the limit $i \to \infty$ (Kawato, 1981; Barbi et al., 1984). Indeed, in the case of the MNT model, relaxation back to the limit cycle after a perturbation is so rapid that these discontinuities appearing on PTC$_1$ are not apparent on PTC$_2$ when t_c is changed in steps of 10 ms (Fig. 7).
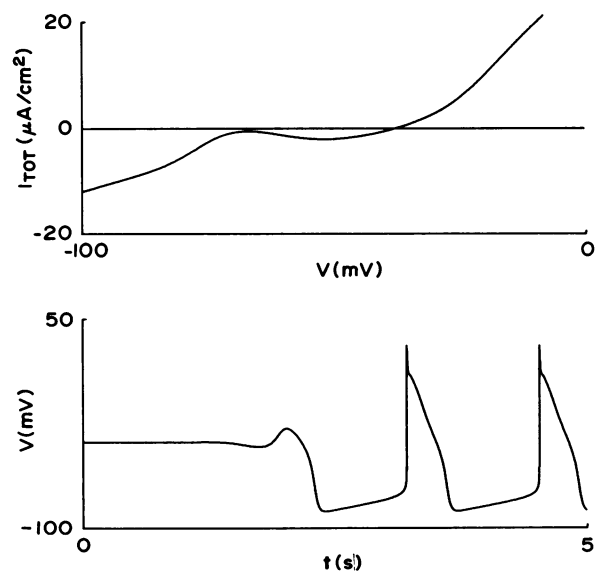
FIGURE 9 Steady-state current–voltage characteristic of MNT equations (top). Note the existence of one and only one zero-current crossing at $V \simeq -37.664$ mV. Evolution of membrane voltage starting with initial conditions appropriate to the steady state at $V = -37.664$ mV (bottom).

increasing even though it remains of degree 1 (e.g., Fig. 7, row 2). There is a very slight downturning in the curve not very evident on the scale of this figure (indicated by the arrow labeled b) just before the abrupt rise in the curve due to the rapid but continuous transition from prolongation to abbreviation of interbeat interval occurring at this current amplitude (Fig. 4, top). For 5 μA/cm^2 $\le A \le$ 11 μA/cm^2, we cannot ascribe a type to PTC$_2$ for reasons described in the Discussion.

When graded action potentials elicited by stimulation during the latter part of repolarization begin to appear (at $A \simeq 7 \mu A/cm^2$), one sees that the membrane potential at the end of the current pulse lies in the plateau range of potentials (Fig. 8). Rather strange-looking, slowly changing membrane responses can then be seen (e.g., Fig. 8; $t_c = 374$ ms). The existence of such responses reinforces the point made earlier about the arbitrariness of the event marker; it also indicates that the definition of an action potential is quite arbitrary.

Fig. 9, top, shows the steady-state current–voltage (IV) characteristic of the MNT model. Note that there is one and only one zero-current crossing of the IV curve: this zero-crossing occurs in the plateau range of potentials. Fig. 9, bottom, shows that starting the numerical integration with all activation and inactivation variables set to the asymptotic values appropriate to the voltage of this steady-state or equilibrium point results in a resumption of spontaneous activity. The steady state is thus unstable, at least to within the numerical resolution of this simulation. Note finally that the slowly changing response of Fig. 8 ($t_c = 374$ ms) is taking place in a voltage range very close to that at which the zero-crossing of the IV curve occurs.

DISCUSSION

The simulations with the MNT model presented above are consistent with experimental reports on the phase resetting of Purkinje fiber with respect to the following main features.

The response is essentially triphasic at low and high pulse amplitudes: a depolarizing stimulus produces a very slight abbreviation in the interbeat interval T_1 if it is applied very early in the cycle (Kass and Tsien, 1976), a prolongation if the same stimulus is applied slightly later in the cycle, and an abbreviation if it is applied sufficiently late (Weidmann, 1951; Jalife and Moe, 1976; Antzelevitch et al., 1982). At low pulse amplitudes, there are two different well-separated ranges of t_c over which prolongation can be seen, with the first (Fig. 3, middle; arrow labeled a) being due to prolongation of action potential duration (Klein et al., 1972; Jalife and Moe, 1976) and the second (Fig. 3, middle; arrow labeled b) being due to prolongation of the duration of diastole (Weidmann, 1951; Jalife and Moe, 1976). This second range occurs just before shortening of the cycle length takes place. At a sufficiently high pulse amplitude, this second range of prolongation is not seen, since the stimulus is then supra-threshold throughout diastole (Weidmann, 1951; Kao and Hoffman, 1958; Klein et al., 1972). Phase-dependent prolongation and shortening of cycle length can also be seen in clinical cases of modulated junctional (Moe et al., 1977) and ventricular (Castellanos et al., 1984) parasystole.

At lower stimulus amplitudes, the maximal degree of prolongation and abbreviation of cycle length attainable

increases with increasing stimulus amplitude (Jalife and Moe, 1976). Longer prolongations might be seen if the MNT model were to be modified by a change that results in a slight outward shift in the IV curve of Fig. 9 in the pacemaker range of potentials. Addition of a net outward current of $<1 \mu A/cm^2$ would convert the system, via a saddle-node bifurcation, into one containing three equilibrium points. In that circumstance, very long prolongations of cycle length showing oscillatory activity in the pacemaker range of potentials similar to those experimentally seen in Purkinje fiber (Klein et al, 1972; Antzelevitch and Moe, 1983) and in heart cell aggregates (Guevara et al., 1986) would then result if the new equilibrium point in the pacemaker range of potentials were to be unstable and have at least one pair of complex conjugate eigenvalues (see also Clay et al., 1984; Reiner and Antzelevitch, 1985).

The transition from prolongation to abbreviation of cycle length occurs at a shorter coupling interval and over an increasingly narrow range of the coupling interval as the stimulus amplitude is increased (Jalife and Moe, 1976; Antzelevitch et al., 1982). In fact, the transition eventually becomes effectively discontinuous (in the presence of membrane noise) at a point midway in the cycle (Jalife and Moe, 1976). We have not investigated at $A = 6 \mu A/cm^2$ (Fig. 4, bottom), using increments of t_c smaller than 0.1 ms, whether or not intermediate responses (similar to those shown in Fig. 4, top) exist at such intermediate pulse amplitudes since it is unlikely that the precision and accuracy of our standard integration scheme suffice under such extreme conditions. However, because of the absence of any equilibrium points (and probably also the stable manifold of the equilibrium point lying in the plateau range of potentials) in the phase space of the MNT system in the pacemaker range of potentials (Fig. 9, top), one might expect that such intermediate responses would be found. The situation is probably similar to that occurring in the Hodgkin–Huxley model of the giant axon of the squid, where increments in the take-off potential of 10^{-12} mV must be used to establish the absence of a true all-or-none depolarization threshold (Clay, 1977). However, such a small change in potential lies well within the membrane voltage noise level of Purkinje fiber. To correctly investigate the existence of all-or-none depolarization would necessitate abandoning the macroscopic Hodgkin–Huxley type of model and instead formulating an inherently stochastic model representing a population of single channels. Note that if the MNT model is modified as outlined above so as to produce three equilibrium points, the presence of an equilibrium point of the saddle type in the phase space of the system would confer upon the membrane the properties of true all-or-none depolarization and repolarization (FitzHugh, 1955, 1960; Clay et al., 1984).

Graded action potentials can be produced by a premature stimulus of sufficiently large amplitude delivered relatively early in the cycle (Weidmann, 1955a; Kao and

Hoffman, 1958; Klein et al., 1972; Jalife and Moe, 1979). Such action potentials will propagate if large enough in amplitude (Kao and Hoffman, 1958). The amplitude, rate of rise of the upstroke, and the overshoot potential of the action potential tend to gradually increase as t_c is increased in both model and experiment. Indeed, for t_c not too small, the overshoot potential and the maximum rate of rise of the upstroke phase are increased beyond their normal values (Weidmann, 1955a; Jalife and Moe, 1976); this effect is not found at lower amplitudes of stimulation (e.g., Fig. 4, *bottom;* t_c = 779.5 ms). Note that while the action potential duration generally tends to increase as t_c increases, there are exceptions (e.g., Fig. 6, t_c = 360 and 380 ms; Fig. 8, t_c = 374 and 384 ms).

Supernormal excitability can be seen in the MNT model (Figs. 5 and 7; see also Fig. 3 of Hauswirth [1971] where a precursor of the MNT model was studied). The behavior shown in Fig. 5 corresponds to supernormal excitability (Weidmann, 1955b; Spear and Moore, 1974; Antzelevitch et al., 1982), since a higher pulse amplitude must be used to elicit an action potential at t_c = 450 or 500 ms (*right*) than to elicit one at a more premature coupling interval of 400 ms (*left*). Supernormality is essentially due to a quicker recovery of threshold potential than of membrane potential (Weidmann, 1951; Spear and Moore, 1974). The existence of supernormal excitability in the MNT model is probably not fortuitous. The quantitative description of many of the currents in that model was formulated from data obtained at an external potassium concentration of 2.6 mM, which is precisely within the range at which supernormal excitability is commonly encountered (Spear and Moore, 1974). When the gap phenomenon occurs, the phase-resetting response becomes quinquephasic, with abbreviation, prolongation, abbreviation, prolongation, and finally abbreviation of cycle length successively being seen as the coupling interval is increased.

The effect on the interbeat interval T_2 of the post-stimulus cycle is generally small, except when graded action potentials are produced in response to a stimulus pulse of very high amplitude. When the duration of the graded action potential is much reduced, the duration T_2 of the post-stimulus or "return" cycle will be very much abbreviated if the duration of diastole is not very much prolonged (Klein et al., 1972). However, the length of the return cycle is variable: for example, the duration of the return cycle can be either shortened or lengthened by a stimulus falling relatively early in the cycle (Klein et al., 1972). Similar findings have been reported in clinical cases of idioventricular rhythm (Kennelly and Lane, 1978). After a graded action potential, the duration of the diastolic period can on occasion be very much prolonged in Purkinje fiber when the stimulus is a propagated wave-front. This leads to a significant increase in the duration of the return cycle, even though the action potential duration is reduced (e.g., Klein et al., 1972). We have not seen such "depression of automaticity" in the MNT model.

Annihilation with a single current pulse is not possible unless some intervention, such as injection of a constant bias current, is carried out (Jalife and Antzelevitch, 1980; Rosenthal and Ferrier, 1983; Chay and Lee, 1984). Also, the equilibrium point at $V \simeq -38$ mV in the MNT model is not stable, in contrast to the statement made in McAllister et al. (1975).

The sign of ΔT_1 is reversed if a hyperpolarizing stimulus is applied instead of a depolarizing stimulus in both the model (Fig. 5 of Hauswirth [1971], reproduced as Fig. 14 of McAllister et al. [1975]) and experiment (Weidmann, 1951; Jalife and Moe, 1976).

Thus, insofar as the transmembrane potential is concerned, the original MNT model does a remarkably good job of accounting for the main features of the phase-resetting experimentally observed. There is only one notable exception to this statement. A maximum prolongation of ~30% (i.e., $T_1/T_0 = 1.3$) can be seen in experiments on Purkinje fiber when a subthreshold pulse is delivered during diastole (Jalife and Moe, 1976, 1979; Antzelevitch et al., 1982). In contrast, a much smaller effect is seen in the MNT model (Fig. 3); in fact, maximal prolongation is then the result of a prolongation of action potential duration and not of diastole. A similar discrepancy between model and experiment has been found in a study of ventricular heart cell aggregates (Clay et al., 1984; Fig. 3). This is perhaps not surprising, since the formulation of the ionic currents active in the pacemaker range of potentials is similar in the two models. It has been recently claimed that modification of the description of the time-dependent pacemaker current can resolve similar discrepancies between model and experiment in the case of the sinoatrial node (Reiner and Antzelevitch, 1985). However, recent work using a model of aggregates of embryonic chick atrial cells (Shrier and Clay, 1986) indicates that the repolarization current kinetics can have a dramatic effect on phase resetting and can generate prolongations in the range of 40% (Shrier and Clay, unpublished observations).

During the decade between the publication of the MNT model and the present time, there has been an accumulation of experimental evidence that has naturally led to the production of revised ionic models of Purkinje fiber (e.g., Drouhard and Roberge, 1982; DiFrancesco and Noble, 1985; Jaeger and Gibbons, 1985). Despite this recent work, the current densities and kinetics of several currents are still uncertain in Purkinje fiber. For example, the sodium current has not been adequately clamped at 37°C, and the details of calcium handling within the cell are largely undetermined. However, it is already known that the reinterpretation of I_{K_2} in terms of I_f makes little or no difference to the phase-resetting effect of a small amplitude pulse delivered during diastole (DiFrancesco and Noble, 1982; Fig. 9). The effect of a reinterpretation of this and other currents (e.g., I_{si}, I_{qr}) on the ionic mechanisms of phase resetting are yet to be completely worked out. In a similar vein, as more accurate descriptions of various

currents become available, the phase-resetting response of newer models will have to be re-investigated.

In some of the studies cited above, phase resetting was carried out in a segment of Purkinje fiber small enough to minimize electrotonic effects (e.g., Jalife and Moe, 1976). However, in other studies, the fiber was long enough so that the influence of the stimulus, a propagating wavefront, would depend in detail upon the cable properties of the Purkinje fiber. Moreover, such long fibers would probably have a pacemaker region somewhere along their length (Weidmann, 1951). The phase-resetting response of a Purkinje fiber of length large in comparison to its space constant is thus very complex; a thorough analysis would involve a study in which the sites of both the recording electrode and the stimulating electrode with respect to the pacemaker region would have to be systematically varied. For example, for stimuli sufficiently premature, one might expect entrance block into the pacemaker region (as commonly occurs in the sinoatrial node). We know of no reports of such systematic studies, and so it is difficult to speculate about phase-resetting in a distributed system where cable properties play an important role.

At a sufficiently low stimulus amplitude, type 1 phase resetting occurs in the MNT model (e.g., Fig. 7, rows 1 and 2); at a sufficiently high stimulus amplitude, type 0 phase resetting occurs (e.g., Fig. 7, rows 5 and 6). Over the intermediate range of stimulus amplitudes ($5 \ \mu A/cm^2 \leq A \leq 11 \ \mu A/cm^2$), the situation is not clear. Over the lower part of this intermediate range ($5 \ \mu A/cm^2 \leq A \leq 7 \ \mu A/cm^2$), an abrupt transition from prolongation to abbreviation of interbeat interval occurs (e.g., Fig. 4, bottom; Fig. 7, row 3). For reasons gone into just above, this transition is probably continuous, though very steep. Should that be the case, type 1 phase resetting would exist. Over the upper part of this intermediate range of stimulus amplitudes ($7 \ \mu A/cm^2 \leq A \leq 11 \ \mu A/cm^2$) a gap phenomenon occurs as the result of a second additional effectively all-or-none abrupt transition (Fig. 5, left). Two correspondingly abrupt jumps can thus be seen in all three plots in row 4 of Fig. 7 at $\phi \simeq 0.34$ (arrows labeled c) and $\phi \simeq 0.41$ (arrows labeled d).

Over the upper part of the intermediate range of stimulus amplitudes ($7 \ \mu A/cm^2 \leq A \leq 11 \ \mu A/cm^2$), there is, in addition, a third range of t_c over which indeterminate behavior occurs. This is seen when graded action potentials first appear (e.g., Fig. 8). At the smallest amplitude where graded action potentials are seen ($A \simeq 7 \ \mu A/cm^2$), the membrane potential at the end of the current pulse lies at ~ -40 mV at the shortest coupling interval that produces an "active" response ($t_c \simeq 370$ ms). This potential is very close to that associated with the equilibrium point (Fig. 9), and a few of the waveforms shown in Fig. 8 resemble the part of the waveform in the lower panel of Fig. 9 at $t \simeq 2$ s. In addition, a wide scatter of responses is found, similar to that shown in row 4 of Fig. 7 ($A = 10 \ \mu A/cm^2$) at $\phi \simeq 0.3$.

This is exactly the type of behavior that one would expect close to the border between type 1 and type 0 phase resetting (Winfree, 1980).

Thus, the results of our work on the MNT equations (Fig. 7, right) indicate that, as the pulse amplitude is increased, one might expect to first see a transition from type 1 phase resetting (rows 1 and 2) to a form of phase resetting to which a type could not be assigned, due to the presence of effectively all-or-none depolarization (row 3). A similar transition has recently been described in spontaneously beating ventricular heart-cell aggregates (Guevara et al., 1986). Further increase of pulse amplitude would result in the appearance of a gap phenomenon (row 4). Again a topological type could not be assigned, due to the presence of two regions of effectively discontinuous behavior. Finally, as pulse amplitude is increased still further, type 0 phase resetting would be encountered (rows 5 and 6).

Two other circumstances have previously been described in cardiac oscillators in which there is not a direct transition from type 1 to type 0 phase resetting. In the first case, as the stimulus amplitude is increased, there is a transition from type 1 phase resetting to a form of resetting to which a type cannot be assigned, because at least one equilibrium point in the system is stable. This results in the possibility of annihilation and triggering of spontaneous activity in Purkinje fiber with a single current pulse (Cranefield and Aronson, 1974; Jalife and Antzelevitch, 1980; Rosenthal and Ferrier, 1983). Note that the standard MNT equations do not support such a response (Fig. 9), unless they are modified in some way (e.g., Chay and Lee, 1984). Annihilation was also not found in two systematic experimental studies on heart cell aggregates (van Meerwijk et al., 1984; Guevara et al., 1986). In the second case, there are three steady states in the system, one of which is a saddle point. As previously mentioned, a very slight outward shift in the total current in the pacemaker range of potentials would suffice to produce such a situation in the MNT model (see Fig. 9, top). In that case, one would again expect a transition from type 1 phase resetting to a form of resetting to which a type could not be ascribed (Clay et al., 1984; Glass and Winfree, 1984). In both of the above cases, one would still however expect to see type 0 phase resetting for a stimulus of sufficiently large amplitude.

While type 1 phase resetting has been clearly demonstrated (e.g., Fig. 5 of Jalife and Moe, 1976), we know of no systematic experimental study in Purkinje fiber investigating the transition from type 1 to type 0 phase resetting. The data shown in Fig. 9 (triangular symbols) of Jalife and Moe (1976) have been interpreted as evidence for type 0 phase resetting (Winfree, 1980). However, the corresponding voltage tracings (Fig. 8 B of Jalife and Moe, 1976) closely resemble those shown in the lower panel of Fig. 4 of this paper, to which we have not been able to ascribe a topological type. A sequence of graded waveforms similar

to that shown in Fig. 5 (*right*) has been described in many studies investigating recovery of action potential duration in Purkinje fiber (e.g., Kao and Hoffman, 1958; Klein et al., 1972). By analogy to the MNT model results (Fig. 7, row *5*), the experimental behavior corresponds to type 0 phase-resetting.

Since type 0 phase resetting does indeed occur in Purkinje fiber as outlined above, the type 1/type 0 border is attainable when stimuli of lower amplitude are delivered. It is precisely stimuli of this order of magnitude that are theoretically needed to produce a rotor, the generative focus of a circulating wave of excitation in one theory for the initiation of ventricular tachycardia (Winfree, 1983). In addition, if a stimulus of effectively the same timing and amplitude as any of those shown in Fig. 4 were to be delivered to a network of Purkinje fibers, a great deal of spatiotemporal inhomogeneity would be produced that could set up optimal conditions for local reentry to occur. It is interesting to note in this respect that the abrupt transition can occur quite late in the cycle for stimuli of not very large amplitude (e.g., Fig. 5, *bottom*) and that there is increasing evidence that episodes of ventricular tachycardia and fibrillation are often provoked in a certain class of patients by premature ventricular contractions falling relatively late in diastole (e.g., Qi et al., 1984). Note that as the stimulus amplitude increases, the region of abrupt transition encroaches on the repolarizing limb of the action potential (Fig. 5, *left;* Fig. 7); this period of time coincides with the so-called "vulnerable phase" where the R-on-T phenomenon occurs (Wiggers and Wegria, 1940; Smirk, 1949). Supernormal excitability would predispose, to an even greater extent than in the above case, to enhanced spatiotemporal inhomogeneity due to the presence of not just one, but rather two, abrupt transitions. It is therefore interesting to note that the incidence of malignant arrhythmias provoked by a train of rapid stimuli was much higher in one study when supernormal excitability existed than when it did not (Harumi et al., 1974). In fact, the close proximity of the phase of supernormality to the vulnerable phase was remarked upon in the original report concerning the R-on-T phenomenon (Smirk, 1949).

A large variety of coupling patterns arises in the MNT model when a periodic train of current pulses, rather than an isolated pulse, is delivered (Guevara, M. R., and A. Shrier, unpublished observations). It has been previously demonstrated in several studies that the phase-resetting response produced by injecting a single stimulus pulse accounts, in large measure, for the various patterns seen during periodic stimulation (Moe et al., 1977; Scott, 1979; Guevara et al., 1981; Glass et al., 1984). In particular, the topological characteristics of the phase-resetting response influence the classes of patterns that can be seen under periodic stimulation in heart cell aggregates (Glass et al., 1984). It remains to be seen whether, in a similar fashion, the topological features of the phase-resetting response of

the MNT model explain the otherwise bewildering array of patterns seen during periodic stimulation.

APPENDIX

In this Appendix, we provide a brief introduction to the mathematical theory of phase resetting (for further background, see Winfree, 1980; Kawato, 1981). The theory developed here is applicable to a system of continuous ordinary differential equations such as the MNT equations. In the MNT equations, the state of the system at any point in time is completely specified by the values of the transmembrane potential V and the nine activation and inactivation variables m, h, d, f, x_1, x_2, q, r, and s. These ten variables can be thought of as defining a ten-dimensional state-point $(V, m, h, d, f, x_1, x_2, q, r, s)$ in the ten-dimensional state-space of the system. Activity then corresponds to movement of the state-point; this motion generates a trajectory. Starting out at time $t = 0$ from almost every set of initial conditions (i.e., values assigned to the ten variables at $t = 0$), the trajectory approaches asymptotically (i.e., for very large times) a closed curve in the ten-dimensional phase space. This closed curve is called a limit cycle, which is said to be stable, since nearby trajectories are attracted to it. Thus, the usual spontaneous action potential generation in the MNT model (Fig. 1, *top*) corresponds to the projection onto the V-axis of the movement of the state-point along the limit cycle.

We can parameterize motion along the limit cycle as follows: choose an arbitrary point on the limit cycle and assign to that point an (old) phase (ϕ) of zero. In our work, we have chosen the point corresponding to -10 mV on the upstroke of the action potential as our $\phi = 0$ reference point. By integrating forward in time for a time t, we can assign an (old) phase of t/T_0 (modulo 1) to any point on the limit cycle, where T_0 is the spontaneous period of oscillation.

Consider now two identical oscillators, whose spontaneous activity is initially synchronous. Injection of a brief stimulus into one of the oscillators will cause, in general, a shift in the relative timing of the two oscillators (e.g., compare top and middle panels of Fig. 1); the perturbed oscillator is said to be phase reset. The magnitude of the phase resetting is quantified by measuring the shift in the time of occurrence of a marker event (in our case the crossing of -10 mV on the action potential upstroke) with respect to an unperturbed control (Fig. 1). As the trajectory asymptotically (i.e., at $t \to \infty$) returns to the limit cycle after a perturbation, these ΔT_i (Fig. 1) approach an asymptotic value. One can define an ith transient phase shift

$$\Delta\phi_i = \Delta T_i/T_0 \quad \text{(modulo 1)} \qquad (A1)$$

and an ith transient new phase

$$\phi_i' = \phi + \Delta T_i/T_0 \quad \text{(modulo 1)}, \qquad (A2)$$

where i is a positive integer. A plot of $\Delta\phi_i$ vs. ϕ is referred to as the ith transient phase response curve (PRC$_i$), whereas a plot of ϕ_i' vs. ϕ is called the ith transient phase transition curve (PTC$_i$). Both $\Delta\phi_i$ and ϕ_i' approach asympotic values as $i \to \infty$. The limiting value of ϕ_i' is called the new or eventual phase, denoted ϕ_∞', whereas a plot of ϕ_∞' vs. ϕ is called the new phase–old phase curve. The rate of convergence of the ΔT_i, $\Delta\phi_i$, and ϕ_i' to their asymptotic values depends on how quickly the trajectory returns to the limit cycle after a perturbation. This rate is very fast in the MNT oscillator, since there are only slight differences between ϕ_2' and ϕ_3'. Thus, one can take ϕ_2' as a good approximation to the eventual phase ϕ_∞'.

When the stimulus amplitude is very small and so the perturbation minimal, one expects that the ΔT_i will be very small, and so from Eq. A2, $\phi_i' \approx \phi$. Thus, a plot of ϕ_2' vs. ϕ will be very close to the diagonal line $\phi_2' = \phi$ (e.g., Fig. 7, row *1*). Its average slope will be one, and so type 1 phase resetting is said to occur. When the stimulus amplitude is very high, one would not expect the ΔT_i to depend on ϕ. Thus, a graph of ϕ_2' vs. ϕ would be expected to yield a curve close to a horizontal straight line. Fig. 7 would

suggest that such an asymptotic curve is being approached in the MNT model as the stimulus amplitude increases. In that case the average slope of the curve is zero, and type 0 phase resetting is said to occur. Note that, by continuity arguments, any limit cycle oscillator is expected to show type 1 phase resetting at a sufficiently low stimulus amplitude, and type 0 phase resetting at a sufficiently high amplitude.

As stimulus amplitude is increased, there is a transition from type 1 to type 0 phase resetting. Since it is impossible to continuously distort a type 1 curve into a type 0 curve, there must be at least one amplitude where there is some sort of discontinuous behavior. This occurs when the state-point of the system at the end of the current pulse lies in the stable manifold of an equilibrium point (of which there is only one in the MNT system; see Fig. 9, top). The stable manifold of an equilibrium point is the set of initial conditions from which a trajectory asymptotically approaches the equilibrium point itself. Thus, for a fixed pulse duration, there will be (at least) one combination of stimulus amplitude and timing for which spontaneous activity will cease as the state-point, lying in the stable manifold, asymptotically approaches the equilibrium point. In that case the eventual phase will be undefined, since the oscillation becomes extinguished. Note that this behavior only occurs in the absence of "noise" in the system, since the equilibrium point is unstable (Fig. 9, bottom). In the presence of noise, the oscillation will restart, but will be reset randomly to some new phase.

REFERENCES

Agha, A. S., A. Castellanos Jr., D. Wells, M. D. Ross, B. Befeler, and R. J. Myerburg. 1973. Type I, type II, and type III gaps in bundle-branch conduction. *Circulation.* 47:325–330.

Antzelevitch, C., and G. K. Moe. 1983. Electrotonic inhibition and summation of impulse conduction in mammalian Purkinje fibers. *Am. J. Physiol.* 245:H42–H53.

Antzelevitch, C., J. Jalife, and G. K. Moe. 1982. Electrotonic modulation of pacemaker activity. Further biological and mathematical observations on the behavior of modulated parasystole. *Circulation.* 66:1225–1232.

Barbi, M., P. G. Haydon, A. V. Holden, and W. Winlow. 1984. On the phase-response curves of repetitively active neurones. *J. Theor. Neurobiol.* 3:15–24.

Castellanos, A., R. M. Luceri, F. Moleiro, D. S. Kayden, R. G. Trohman, L. Zaman, and R. J. Myerburg. 1984. Annihilation, entrainment and modulation of ventricular parasystolic rhythms. *Am. J. Cardiol.* 54:317–322.

Chay, T. R., and Y. S. Lee. 1984. Impulse responses of automaticity in the Purkinje fiber. *Biophys. J.* 45:841–849.

Clay, J. R. 1977. Monte Carlo simulation of membrane noise: an analysis of fluctuations in graded excitation of nerve membrane. *J. Theor. Biol.* 64:671–680.

Clay, J. R., M. R. Guevara, and A. Shrier. 1984. Phase resetting of the rhythmic activity of embryonic heart cell aggregates. Experiment and theory. *Biophys. J.* 45:699–714.

Cranefield, P. F., and R. S. Aronson. 1974. Initiation of sustained

rhythmic activity by single propagated action potentials in canine cardiac Purkinje fibres exposed to sodium-free solution or to ouabain. *Circ. Res.* 34:477–481.

DiFrancesco, D., and D. Noble. 1982. Implications of the re-interpretation of i_{K_2} for the modelling of the electrical activity of pacemaker in the heart. *In* Cardiac Rate and Rhythm. L. N. Bouman and H. J. Jongsma, editors. Martinus Nijhoff Publishers, The Hague, Netherlands. 93–128.

DiFrancesco, D., and D. Noble. 1985. A model of cardiac electrical activity incorporating ionic pumps and concentration changes. *Philos. Trans. R. Soc. Lond. Biol. Sci.* 307:353–398.

Drouhard, J. P., and F. A. Roberge. 1982. The simulation of repolarization events of the cardiac Purkinje fiber action potential. *IEEE (Inst. Electr. Electron. Eng.) Trans. Biomed. Eng.* BME-29:481–483.

FitzHugh, R. 1955. Mathematical models of threshold phenomena in the nerve membrane. *Bull. Math. Biophys.* 17:257–278.

FitzHugh, R. 1960. Thresholds and plateaus in the Hodgkin-Huxley nerve equations. *J. Gen. Physiol.* 43:867–896.

Glass, L., and A. T. Winfree. 1984. Discontinuities in phase-resetting experiments. *Am. J. Physiol.* 246:R251–R258.

Glass, L., M. R. Guevara, J. Belair, and A. Shrier. 1984. Global bifurcations of a periodically forced biological oscillator. *Phys. Rev. A.* 29:1348–1357.

Guevara, M. R., L. Glass, and A. Shrier. 1981. Phase locking, period-doubling bifurcations, and irregular dynamics in periodically stimulated cardiac cells. *Science (Wash. DC).* 214:135–1353.

Guevara, M. R., A. Shrier, and L. Glass. 1986. Phase resetting of spontaneously beating embryonic ventricular heart cell aggregates. *Am. J. Physiol.* 251:H1298–H1305.

Harumi, K., J. Owens, M. J. Burgess, and J. A. Abildskov. 1974. Relationship of ventricular excitability characteristics to ventricular arrhythmias in dogs. *Circ. Res.* 35:464–471.

Hauswirth, O. 1971. Computer-rekonstruktionen der Effekte von Polarisationsströmen und Pharmaka auf Schrittmacher- und Aktionspotentiale von Herzmuskelfasern. Habilitationsschrift. Ruprecht-Karl-Universitat, Heidelberg.

Jaeger, J. M., and W. R. Gibbons. 1985. Slow inward current may produce many results attributed to I_{x_1} in cardiac Purkinje fibers. *Am. J. Physiol.* 249:H122–H132.

Jalife, J., and C. Antzelevitch. 1980. Pacemaker annihilation: diagnostic and therapeutic implications. *Am. Heart J.* 100:128–129.

Jalife, J., and G. K. Moe. 1976. Effect of electronic potentials on pacemaker activity of canine Purkinje fibers in relation to parasystole. *Circ. Res.* 39:801–808.

Jalife, J., and G. K. Moe. 1979. A biologic model of parasystole. *Am. J. Cardiol.* 43:761–772.

Kao, C. Y., and B. F. Hoffman. 1958. Graded and decremental response in heart muscle fibers. *Am. J. Physiol.* 194:187–196.

Kass, R. S., and R. W. Tsien. 1976. Control of action potential duration by calcium ions in cardiac Purkinje fibers. *J. Gen. Physiol.* 67:599–617.

Kawato, M. 1981. Transient and steady state phase response curves of limit cycle oscillators. *J. Math. Biol.* 12:13–30.

Kennelly, B. M., and G. K. Lane. 1978. Effect of ventricular extrasystoles on idioventricular rhythm in patients with complete heart block. *Cardiovasc. Res.* 12:703–711.

Klein, H. O., P. F. Cranefield, and B. F. Hoffman. 1972. Effect of extrasystoles on idioventricular rhythm. *Circ. Res.* 30:651–665.

McAllister, R. E., D. Noble, and R. W. Tsien. 1975. Reconstruction of the electrical activity of cardiac Purkinje fibres. *J. Physiol. (Lond.).* 251:1–59.

Moe, G. K., J. Jalife, W. J. Mueller, and B. Moe. 1977. A mathematical model of parasystole and its application to clinical arrhythmias. *Circulation.* 56:968–979.

Pavlidis, T. 1973. Biological Oscillators: Their Mathematical Analysis. Academic Press, Inc., New York.

Qi, W. H., N. S. Fineberg, and B. Surawicz. 1984. The timing of

ventricular premature complexes initiating chronic ventricular tachy-cardia. *J. Electrocardiol. (San Diego).* 17:377–384.

Reiner, V. S., and C. Antzelevitch. 1985. Phase resetting and annihilation in a mathematical model of sinus node. *Am. J. Physiol.* 249:H1143–H1153.

Rosenthal, J. E., and G. R. Ferrier. 1983. Contribution of variable entrance and exit block in protected foci to arrhythmogenesis in isolated ventricular tissues. *Circulation.* 67:1–8.

Scott, S. W. 1979. Stimulation simulations of young yet cultured beating hearts. Ph.D. Dissertation. State University of New York at Buffalo, Buffalo, NY.

Shrier, A., and J. R. Clay. 1986. Repolarization currents in embryonic chick atrial heart cell aggregates. *Biophys. J.* 50:861–874.

Smirk, F. H. 1949. R waves interrupting T waves. *Br. Heart J.* 11:23–36.

Spear, J. R., and E. N. Moore. 1974. Supernormal excitability and conduction in the His-Purkinje system of the dog. *Circ. Res.* 35:782–792.

van Meerwijk, W. P. M., G. de Bruin, A. C. G. van Ginneken, J. van Hartevelt, H. J. Jongsma, E. W. Kruyt, S. S. Scott, and D. L. Ypey.

1984. Phase resetting properties of cardiac pacemaker cells. *J. Gen. Physiol.* 83:613–629.

Victorri, B., A. Vinet, F. A. Roberge, and J.-P. Drouhard. 1985. Numerical integration in the reconstruction of cardiac action potentials using Hodgkin-Huxley-type models. *Comp. Biomed. Res.* 18:10–23.

Weidmann, S. 1951. Effect of current flow on the membrane potential of cardiac muscle. *J. Physiol. (Lond.).* 115:227–236.

Weidmann, S. 1955a. The effect of the cardiac membrane potential on the rapid availability of the sodium-carrying system. *J. Physiol. (Lond.).* 127:213–224.

Weidmann, S. 1955b. Effects of calcium ions and local anaesthetics on electrical properties of Purkinje fibres. *J. Physiol. (Lond.).* 129:568–582.

Wiggers, C. J., and R. Wegria. 1940. Ventricular fibrillation due to single, localized induction and condenser shocks applied during the vulnerable phase of ventricular systole. *Am. J. Physiol.* 128:500–505.

Winfree, A. T. 1980. The Geometry of Biological Time. Springer-Verlag, New York.

Winfree, A. T. 1983. Sudden cardiac death: a problem in topology. *Sci. Am.* 248(No. 5):144–161.